1 Chapter 1. Flow

Scope. We introduce the flow model and define phase as its measure. We recall quaternions, state why we use them, and explain when a complex slice is used. We then introduce three angles—intrinsic (ζ), gravitational (ϕ), and kinematic (ϑ)—and state the SR simplification.

1.1 1.1. The spatially-linked quaternion

Let $q(\mathbf{x}, t) \in S^3 \simeq SU(2)$ denote the flow state. Fix an *internal* imaginary basis $\{I, J, K\} \subset \Im\mathbb{H}$. The observed (lab) orthonormal triad is the conjugated image

$$\mathbf{e}_I(q) = qIq^{-1}, \qquad \mathbf{e}_J(q) = qJq^{-1}, \qquad \mathbf{e}_K(q) = qKq^{-1}. \tag{1.1}$$

The *time fiber* is generated by right multiplication with $e^{\frac{\phi}{2}K}$; its spatial director (shadow) is $\mathbf{n}(q) = qKq^{-1} \in S^2$.

1.2 1.2. Why quaternion algebra

Quaternions form the minimal non-commutative algebra that: (i) double-covers $SO(3)$ for rigid 3D rotations; (ii) carries the Hopf fibration $S^3 \to S^2$, separating an internal S^1 time fiber from spatial orientations; and (iii) encodes non-commutativity necessary for Wigner–Thomas rotations (residual spatial rotations from composing non-collinear boosts). (Hopf [1]; Wigner [3]; Thomas [2]).

1.3 1.3. Why (and where) we use a complex slice

For exposition we sometimes restrict to the commuting slice span$\{1, K\} \cong \mathbb{C}$, which preserves the time fiber while suppressing transverse components. We use this slice in SR derivations and in phase-1-form preliminaries; non-collinear compositions revert to the full quaternionic picture.

1.4 1.4. Three angles

We introduce three angles with distinct roles:

- **Intrinsic tilt** $\zeta \in [0, \frac{\pi}{2}]$: angle between the flow tangent and the time fiber. It controls optical and evolutionary ("Friedmann-like") effects of the same flow:

$$v_{\mathrm{ph}} = ccos\zeta, \qquad n(\zeta) = \frac{c}{v_{\mathrm{ph}}} = \sec\zeta, \qquad \frac{d\tau}{dt} = cos\zeta. \tag{1.2}$$

- **Gravitational angle** ϕ: an *external* flow-induced tilt field. In the weak, stationary regime it encodes Schwarzschild-like clock and light effects via an effective index $n_g = \sec\phi$ and time-rate $d\tau/dt = \cos\phi$. We do not build full field equations here.

- **Kinematic angle** ϑ: SR angle for relative motion between comoving flows:

$$\beta = sin\vartheta, \qquad \gamma = \sec\vartheta, \qquad \tanh\eta = sin\vartheta. \tag{1.3}$$

1.5 1.5. SR simplification

Whenever two objects share $\zeta_A = \zeta_B$ and $\phi_A = \phi_B$ along a worldline segment, a local comoving frame exists where SR applies. In SR-focused chapters we adopt $\zeta = \phi = 0$ and retain only the kinematic angle ϑ.

2 Chapter 2. The kinematic angle

2.1 2.1. Definition

Define ϑ so that SR kinematics lives on a circle rather than a hyperbola:

$$\beta = sin\vartheta, \qquad \gamma = \sec\vartheta, \qquad \tanh\eta = sin\vartheta, \qquad cosh\eta = \sec\vartheta. \tag{2.1}$$

2.2 2.2. Mapping and correspondence

oindent*See also Fig. 1.*

Quantity	Standard SR (hyperbolic)	Phase picture (circular)
Rapidity	η	$\tanh\eta = \sin\vartheta$
Lorentz factor	$\gamma = \cosh\eta$	$\gamma = \sec\vartheta$
Speed	$\beta = \tanh\eta$	$\beta = \sin\vartheta$
Longitudinal Doppler	$k = e^{\pm\eta}$	$k = \dfrac{1+\tan(\vartheta/2)}{1-\tan(\vartheta/2)}$
Temporal projection	$\operatorname{sech}\eta$	$\cos\vartheta$

Table 1: SR–phase correspondences for the kinematic angle.

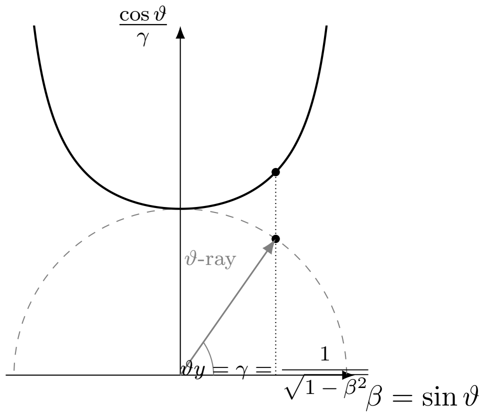

Figure 1: Phase circle vs. Lorentz hyperbola at common $\beta = \sin\vartheta$. Vertical mapping at fixed β illustrates the Gudermann bridge: $\gamma = \sec\vartheta = \cosh\eta$. See mapping in Table 1.

3 Time and space as phase derivatives

Why a complex slice of a quaternion? For local kinematics any unit direction $\hat{\mathbf{u}}$ singles out the two–dimensional subalgebra $\mathrm{Span}\{1, \hat{\mathbf{u}}\} \cong \mathbb{C} \subset \mathbb{H}$. Working in this complex *slice* preserves all boost/rotation algebra along $\hat{\mathbf{u}}$, but keeps formulas elementary. When the direction changes, one updates the slice; the full quaternionic structure is retained.

Let $\vec{\chi} \in \mathbb{C}$ be a variable whose change generates observable time-space effects. We treat the time and space units as directional derivatives (phase velocities) along the real and imaginary directions of a complex basis $(\hat{h}, \mathbf{l})$:

$$\hat{h}\, dx_0 = \frac{\partial\vec{\chi}}{\partial\chi_h}\frac{d\chi_h}{d\chi}\, d\chi = \tilde{H}\, d\chi, \qquad \mathbf{l}\, dx_l = \frac{\partial\vec{\chi}}{\partial\chi_l}\frac{d\chi_l}{d\chi}\, d\chi = \tilde{L}\, d\chi, \quad l = 1, 2, 3. \tag{3.1}$$

Introduce the phase speed of the SR interval $ds = \tilde{S}\,d\chi$. The interval conservation takes the form

$$\tilde{S}^2 = \frac{ds^2}{d\chi^2} = \frac{g_{ij}\,dx^i dx^j}{d\chi^2} = \left(\frac{\mathsf{c}^2 dt^2}{d\chi^2}\right) - \left[\frac{\mathbf{dx}^2}{d\chi^2}\right] = \left(\tilde{H}^2\right) - \left[\tilde{L}^2\right], \tag{3.2}$$

equivalently

$$\tilde{H}^2 = \tilde{S}^2 + \tilde{L}^2. \tag{3.3}$$

Writing

$$\tilde{S} = \tilde{H}cos\theta, \qquad \tilde{L} = \tilde{H}sin\theta, \tag{3.4}$$

where θ is the angle of the phase speed relative to the real axis. Algebraically, (3.3) is a Euclidean decomposition of a single speed into orthogonal projections; physically, we will see that under reparameterization the *projection* $\tilde{S}$, not the Euclidean norm $\tilde{H}$, is the conserved Minkowski quantity.

Flow and phase 1-form. Let $\Phi : \mathcal{E} \to \mathbb{R}$ be a scalar *phase potential* on a (possibly infinite-dimensional) Euclidean/Hilbert proto-space $(\mathcal{E}, \langle\cdot,\cdot\rangle)$. Define the phase 1-form $\alpha := d\Phi$ and the associated *flow vector* $\boldsymbol{\chi} := abla\Phi$, where the gradient is taken with respect to $\langle\cdot,\cdot\rangle$.

Fix an observer's orthonormal spatial triad $\{\mathbf{e}_1, \mathbf{e}_2, \mathbf{e}_3\} \subset \mathcal{E}$ and let $S = \operatorname{span}\{\mathbf{e}_1, \mathbf{e}_2, \mathbf{e}_3\}$ with orthogonal projectors P_S and $P_{S^\perp}$. Decompose

$$\boldsymbol{\chi} = \boldsymbol{\chi}_S + \boldsymbol{\chi}_\perp, \qquad \boldsymbol{\chi}_S := P_S\boldsymbol{\chi}, \quad \boldsymbol{\chi}_\perp := P_{S^\perp}\boldsymbol{\chi}.$$

Define observable spatial components and the orthogonal magnitude

$$\ell_i := \langle\boldsymbol{\chi}, \mathbf{e}_i\rangle, \qquad \mathbf{l} := \sum_{i=1}^{3} \ell_i\,\mathbf{e}_i, \qquad t := \|\boldsymbol{\chi}_\perp\| = \sqrt{\|\boldsymbol{\chi}\|^2 - \|\boldsymbol{\chi}_S\|^2},$$

and, for orientation when $t > 0$, the unit direction $\mathbf{e}_t := \boldsymbol{\chi}_\perp/\|\boldsymbol{\chi}_\perp\|$. Then the phase angle ϑ and the direction $\mathbf{u}$ used throughout this paper are recovered as

$$\cos\vartheta = \frac{t}{\|\boldsymbol{\chi}\|}, \qquad \sin\vartheta = \frac{\|\mathbf{l}\|}{\|\boldsymbol{\chi}\|}, \qquad \mathbf{u} = \frac{\mathbf{l}}{\|\mathbf{l}\|} \quad (\|\mathbf{l}\| > 0).$$

This complements the operational definition (**??**) and ties the phase picture to a differential-form language.

4 Phase space

Let the phase vector space be $\mathbb{H}$ with orthonormal basis $(\hat{h}, \mathbf{l})$. For a phase vector $\vec{\chi} = R\,e^{\theta\mathbf{l}}$ with $\theta \in [-\pi, \pi]$,

$$\tilde{H} = R, \qquad \tilde{S} = Rcos\theta, \qquad \tilde{L} = R\,\mathbf{l}sin\theta. \tag{4.1}$$

Choosing coordinates where the projectors onto $(\hat{h}, \mathbf{l})$ are unit, (3.1) simplifies to

$$\hat{h}\,dx_0 = \frac{d\chi_h}{d\chi}\,d\chi = \tilde{H}\,d\chi, \qquad \mathbf{l}\,dx_l = \frac{d\chi_l}{d\chi}\,d\chi = \tilde{L}\,d\chi. \tag{4.2}$$

The map from phase to observables is an integral transform:

$$x^i(\chi) = x^i(\chi_0) + \int_{\chi_0}^{\chi} \tilde{X}^i(u)\,du, \qquad i = 0, 1, 2, 3, \tag{4.3}$$

where $\tilde{X}^i$ are projections of $d\vec{\chi}/d\chi$ onto $(\hat{h}, \mathbf{l})$ and $x^i(\chi_0)$ fix initial conditions.

5 Objects

oindent*Roadmap.* The next formulas fix notation and the geometric carriers we use throughout. In particular, the phase state $(\vartheta, \mathbf{u})$ selects a complex slice $\mathbb{C}_{\mathbf{u}} \subset \mathbb{H}$; collinear compositions become ordinary circular sums on this slice, while non-collinear compositions generate a genuine 3D rotation (Wigner–Thomas) via quaternion multiplication. This explains why we keep both ϑ and $\mathbf{u}$ as primary objects.

A fundamental particle is an elementary object with nonzero phase $\vec{\chi}eq0$. Composite objects are phase configurations; to represent them in phase space one may require additional dimensions, except for the photon, whose phase is always aligned with the imaginary axis:

$$\mathbf{p} = \frac{d\vec{\chi}}{d\chi_l} = p\,\mathbf{l} \in \Im. \tag{5.1}$$

Non-photonic phenomena are associated with nonzero real projection and nonzero mass. A complex object can be identified with an event or worldline; the photon corresponds to a null-interval point encoding information about the event.

Any object's phase can be rotated to the *zero* (purely real) direction,

$$\vec{\chi}_0 = R \in \Re. \tag{5.2}$$

An object A moving with speed v relative to a rest observer has

$$\vec{\chi}_A = R\, e^{\vartheta_A \mathbf{l}}, \qquad sin\vartheta_A = \frac{v}{\mathsf{c}} \equiv \beta. \tag{5.3}$$

oindent*From unit norm to the interval.* We will repeatedly use that $cd\tau = c\,dt\,\cos\vartheta$ and $d\mathbf{x} = c\,dt\,\sin\vartheta\,\mathbf{u}$. Thus the identity $\cos^2\vartheta + \sin^2\vartheta = 1$ is exactly the Minkowski metric statement $(cd\tau)^2 = (cdt)^2 - d\mathbf{x}^2$; from now on, square-root expressions are traded for circular trigonometry in ϑ.

5.1 Space as a symmetric phase pair

From (3.4), a naive zero-angle limit would remove the imaginary projection, contradicting observability. We enforce a nonvanishing spatial projection by pairing opposite-phase tilts:

$$\vec{\chi}^{\pm} = R\, e^{\pm\zeta\mathbf{l}}, \qquad \vec{\chi}_l := \frac{\vec{\chi}^{+} - \vec{\chi}^{-}}{2} = R\,\mathbf{l} sin\zeta, \tag{5.4}$$

where ζ is an *internal angle* (intrinsic to the object; heuristically linked to mass/density). The local decomposition is

$$\vec{\chi}_0 = \vec{\chi}_\tau + \vec{\chi}_l = Rcos\zeta + R\,\mathbf{l} sin\zeta, \tag{5.5}$$

with unit components (normalized by R): the real component is $\cos\zeta$ and the imaginary component is $\sin\zeta$.

5.2 Absolute, local, and observed time

Define *absolute* time $t = t(\tilde{H})$ at the zero phase direction; it is the fastest clock and useful for normalization between different phase speeds. Along the local real direction,

$$dx_0 = \frac{d}{d\chi}\Re(\vec{\chi})\, d\chi = \frac{\vec{\chi}^{+} + \vec{\chi}^{-}}{2}\, d\chi = cos\zeta\, d\chi =: d\tau. \tag{5.6}$$

Here $d\chi_0 := \cos\zeta\, d\chi$ is the projection of $d\chi$ onto the local real axis; in Sec. 5.3 we calibrate $d\tau = (1/u_0)\, d\chi_0$. The observed proper time of A relative to the rest observer is

$$\tilde{H}_A = \Re\left(\frac{d\vec{\chi}_A}{d\vec{\chi}_0}\right) = cos\vartheta_A = \sqrt{1 - sin^2\vartheta_A} = \sqrt{1 - \frac{v^2}{\mathsf{c}^2}} = \frac{1}{\gamma}. \tag{5.7}$$

5.3 Normalization

oindent *Calibration.* We fix the calibration by the observer's clock and speed budget: $\cos\vartheta \equiv d\tau/dt$ and $\sin\vartheta \equiv \beta$. This choice does not restrict generality: any overall rescaling of the underlying flow is absorbed into the definitions of t and c, leaving all dimensionless observables unchanged.

Let local time be parameterized by *phase*; introduce a reference frequency u_0 and set

$$d\tau = \frac{1}{u_0}\, d\chi_0. \tag{5.8}$$

By the chain rule,

$$dx_0 = \tilde{H}\, d\chi = \frac{dx_0}{d\chi_0}\frac{d\chi_0}{d\tau}\, d\tau = \tilde{H}\,\dot{\chi}\, d\tau =: \dot{H}\, d\tau, \tag{5.9}$$

where $u := d\chi/d\tau$, $\dot{\chi} := u/u_0$, and $\dot{H} := \tilde{H}\,\dot{\chi}$. Choosing the calibration $\dot{H} \equiv \mathsf{c}$ gives $dx_0 = \mathsf{c}\, d\tau$. Similarly for space,

$$dx_l = \tilde{L}\, d\chi = \frac{dx_l}{d\chi_0}\frac{d\chi_0}{dl}\, dl = \tilde{L}\,\chi'\, dl =: L'\, dl, \qquad \chi' := \frac{d\chi}{dl}. \tag{5.10}$$

From $dx_0 = dx_l$ for light one gets

$$\mathsf{c} = \tilde{L}'\,\frac{dl}{d\tau}, \tag{5.11}$$

hence with temporal calibration to c the spatial scale becomes unit: $\tilde{L}' = 1$.

5.4 Light and c as a calibration constant

From the normalized forms,

$$\frac{\mathsf{c}}{\dot{\chi}}\, d\chi = \frac{1}{\chi'}\, d\chi \quad\Rightarrow\quad \mathsf{c} = \frac{\dot{\chi}}{\chi'} = \frac{dl}{d\tau}, \tag{5.12}$$

i.e. c is a *calibration constant* tying temporal and spatial measures, independent of local phase variation. Equation (7.12) also reads

$$\mathsf{c} = \left(\frac{d\chi}{d\tau}\right)\left[\frac{dl}{d\chi}\right] \sim (u)\,[\lambda], \tag{5.13}$$

matching frequency and wavelength of a photon, with χ as its phase. For a lightlike trajectory,

$$ds^2 = \mathsf{c}^2\left(\frac{d\chi^2}{\dot{\chi}^2} - \frac{d\chi^2}{\dot{\chi}^2}\right) = 0. \tag{5.14}$$

At unit frequency, $\tau = \chi$: the photon's "proper time" is its phase, and the length of its phase-speed vector equals its wavelength, $\tilde{H}_p = \lambda$. Finally, the kinematic slope in phase coordinates is

$$\frac{dx_l}{dx_0} = \frac{\tilde{L}\, d\chi}{\tilde{H}\, d\chi} = \sin\vartheta = \frac{v}{\mathsf{c}} \equiv \beta, \tag{5.15}$$

so $\vartheta = \pi/2$ implies $v = \mathsf{c}$.

5.5 Lorentz factor via reparameterization

A change of direction of the phase speed transforms

$$\tilde{H}^2 = \tilde{S}^2 + \tilde{L}^2 \longmapsto \dot{H}^2 = \dot{S}^2 + \dot{L}^2. \tag{5.16}$$

Lemma (parameter-change identity). The transition $\tilde{H} \to \dot{S}$ is the manifestation of evolving phase speed under the parameter change $\chi \mapsto \tau(\chi)$, with local Jacobian

$$\frac{d\tau}{d\chi} = \cos\zeta(\chi)\cos\vartheta(\chi) \quad \Rightarrow \quad \mathcal{J}(\zeta,\vartheta) := \frac{d\chi}{d\tau} = \frac{1}{\cos\zeta\,\cos\vartheta}. \tag{5.17}$$

Then

$$\dot{H} = \tilde{H}\,\mathcal{J}, \qquad \dot{L} = \tilde{L}\,\mathcal{J}. \tag{5.18}$$

In differential form,

$$d\ln\dot{H} = d\ln\mathcal{J} = \tan\zeta\,d\zeta + \tan\vartheta\,d\vartheta. \tag{5.19}$$

For a *pure boost* ($d\zeta = 0$) one has $d\dot{H} = \dot{H}\tan\vartheta\,d\vartheta$. Absorbing a constant $cos\zeta$ into the calibration (set $\zeta = 0$ henceforth), we obtain

$$\tilde{H}^2 = \dot{H}^2 - \dot{L}^2 = \sec^2\vartheta\,(\tilde{H}^2 - \tilde{L}^2) = \gamma^2(\tilde{H}^2 - \tilde{L}^2). \tag{5.20}$$

Corollary. In phase space the Euclidean norm $\tilde{H}$ is conserved; in observed time the Minkowski norm $\dot{S}$ is conserved; they are identical as quantities:

$$\boxed{\tilde{H} = \dot{S}}. \tag{5.21}$$

5.6 Rapidity and the phase angle

By definition,

$$\beta = \frac{v}{\mathsf{c}} = \sin\vartheta, \qquad \tanh\eta = \beta, \qquad d\eta = \frac{d\beta}{1-\beta^2}. \tag{5.22}$$

With $d\beta = cos\vartheta\,d\vartheta$ and $1-\beta^2 = cos^2\vartheta$,

$$d\eta = \sec\vartheta\,d\vartheta, \qquad \eta(\vartheta) = \int \sec\vartheta\,d\vartheta = \ln|\sec\vartheta + \tan\vartheta| = \tfrac{1}{2}\ln\frac{|1+\sin\vartheta|}{|1-\sin\vartheta|}. \tag{5.23}$$

Fixing $\eta(0) = 0$,

$$e^{\eta(\vartheta)} = \sqrt{\frac{1+\sin\vartheta}{1-\sin\vartheta}}, \qquad \gamma = \frac{1}{\sqrt{1-\beta^2}} = \sec\vartheta = \cosh\eta. \tag{5.24}$$

Remark (groups). Observables satisfy $\beta = sin\vartheta = \tanh\eta$ and $\gamma = \sec\vartheta = cosh\eta$. Thus Euclidean rotations in the phase circle ($U(1)$ with angle ϑ) reproduce the numerical factors of hyperbolic boosts in $SO^+(1,1)$ (rapidity η) *after* reparameterizing time. We do not claim an isomorphism $U(1) \cong SO(1,1)$; only the equality of observable combinations under the change of parameter.

5.7 Velocity addition

Notation. In unimetry, an inertial boost is a *D-rotation*

$$\mathcal{B}(\hat{\mathbf{u}},\psi): \quad \mathbf{q} \mapsto d\,\mathbf{q}\,d, \qquad d = \cos\frac{\psi}{2} + \hat{\mathbf{u}}\sin\frac{\psi}{2}, \tag{5.25}$$

and a spatial rotation is an *R-rotation*

$$\mathcal{R}(\hat{\mathbf{n}},\phi): \quad \mathbf{q} \mapsto r\,\mathbf{q}\,r^{-1}, \qquad r = \cos\frac{\phi}{2} + \hat{\mathbf{n}}\sin\frac{\phi}{2}. \tag{5.26}$$

Kinematic mapping: $\beta \equiv v/c = sin\psi$, $\gamma = 1/cos\psi$, $\tan\dfrac{\psi}{2} = \dfrac{\gamma\beta}{\gamma+1}$. For quaternionic/GA accounts of rotors and Lorentz boosts see [**?**, **?**, **?**].

5.7.1 Wigner rotation

Let d_1, d_2 be D-rotors of two successive boosts. The raw action on any unimetry 4-object is

$$\mathbf{q}' = d_2 d_1\, \mathbf{q}\, d_1 d_2 \equiv L_{12}\, \mathbf{q}\, L_{21}, \qquad L_{12} = d_2 d_1, \quad L_{21} = d_1 d_2. \tag{5.27}$$

Define d_{12} to be the unique D-rotor reproducing the combined spatio–temporal tilt of L_{12}:

$$\boxed{d_{12}\, \mathbf{e}_t\, d_{12} \;=\; L_{12}\, \mathbf{e}_t\, L_{21}, \qquad \Re(d_{12}) \geq 0} \tag{5.28}$$

(the sign choice removes the trivial two-fold ambiguity). Then the *Wigner rotor* is the residual R-rotation in the symmetric D–R factorization:

$$\boxed{L_{12} = d_{12}\, r_W, \qquad L_{21} = r_W^{-1}\, d_{12}} \tag{5.29}$$

equivalently,

$$\boxed{r_W = \bar{d}_{12}\, L_{12} = L_{21}\, \bar{d}_{12}}. \tag{5.30}$$

Hence the observed map after compensating the tilt is $\bar{d}_{12}\, \mathbf{q}'\, \bar{d}_{12} = r_W\, \mathbf{q}\, r_W^{-1}$.

$$\begin{tikzcd}
\mathbf{q} \arrow[r, "d_1"] \arrow[rr, dashed, bend left, "d_{12}"] & d_1\, \mathbf{q}\, d_1 \arrow[r, "d_2"] & d_2 d_1\, \mathbf{q}\, d_1 d_2 \arrow[d, "\bar{d}_{12} \text{ on both sides}"] \\
 & & r_W\, \mathbf{q}\, r_W^{-1}
\end{tikzcd}$$

Figure 2: Two successive D-rotations (boosts) and compensation of the net spatio–temporal angle by the conjugate of d_{12}, leaving a pure R-rotation r_W.

Legend (phase circle ↔ hyperbolic plane):

$$\beta = \tanh\eta = sin\vartheta, \quad \gamma = cosh\eta = \sec\vartheta, \quad k_\parallel = e^{\pm\eta} = \frac{1+\tan(\vartheta/2)}{1-\tan(\vartheta/2)}.$$

6 Chapter 3. Time and space as derivatives

Concept. Time and space are derived observables from the phase flow.

6.1 3.1. Flow via a phase 1-form

Let the phase be a 1-form $\alpha = d\phi$. Its curvature is the 2-form $F = d\alpha$. With energy stiffness κ defined by $E = \kappa c^3$, the energy current is

$$J_E = \star(\kappa\, \alpha), \qquad dJ_E = 0 \;\; \text{(free flow)}, \tag{6.1}$$

so that exchanges obey $dJ_E eq0 \Leftrightarrow \dot{\kappa} eq0$. In observed 3D the director field $\mathbf{n} = qKq^{-1}$ drives dynamics via

$$\mathbf{a} = c^2\, abla \times \mathbf{n}, \qquad \mathbf{F} = E\, abla \times \mathbf{n}, \qquad m = \kappa c. \tag{6.2}$$

Optics of the same flow follows from ζ: $v_{\text{ph}} = ccos\zeta$, $n = \sec\zeta$, hence $\varepsilon_{\text{flow}}\mu_{\text{flow}} = n^2/c^2$.

6.2 3.2. The spatially-linked quaternion (formal)

The lab triad is reconstructed from the internal basis by conjugation: $\mathbf{e}_{I,J,K}(q) = q\,(I, J, K)\,q^{-1}$. The time fiber is generated by right-multiplication with $e^{\frac{\phi}{2}K}$. D-tilts (boosts) along $V \perp K$ act as

$$q \;\mapsto\; e^{\frac{\eta}{2}V}\,q\,e^{\frac{\eta}{2}V}, \qquad \tanh\eta = \sin\vartheta. \tag{6.3}$$

Successive non-collinear D-tilts generate Wigner rotations (see Appendix).

6.3 3.3. A reminder on the Hopf fibration

The Hopf connection α_H and curvature satisfy

$$\alpha_H = \tfrac{1}{2}\langle K,\, 2\,\mathrm{Im}(q^{-1}dq)\rangle, \qquad d\alpha_H = \tfrac{1}{2}\,\mathbf{n}\cdot(d\mathbf{n}\wedge d\mathbf{n}), \tag{6.4}$$

identifying curvature with the area 2-form on S^2. See Hopf [1]. Residual rotations from non-commuting boosts are the holonomy of this connection.

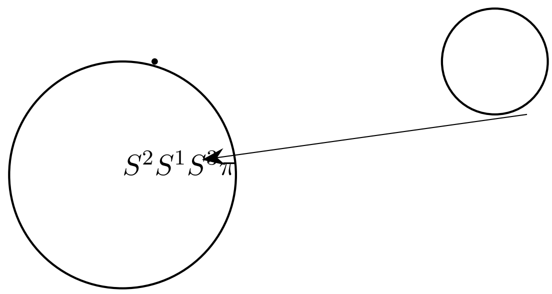

Figure 3: Hopf fibration $S^3 \xrightarrow{\pi} S^2$: each base point carries a circular fiber S^1. The director $\mathbf{n}(q) = qKq^{-1}$ lives on S^2, while motion along the fiber encodes gauge time.

6.4 3.4. The "quantum quaternion" (placeholder)

Here we only set notation: by "quantum quaternion" we mean the flow state endowed with a Hilbert-space structure over the complex slice span$\{1, K\}$, suitable for spinor representations and Berry phases [4]. Full QM linkage is deferred to a separate paper.

7 Objects

oindent*Roadmap.* The next formulas fix notation and the geometric carriers we use throughout. In particular, the phase state $(\vartheta, \mathbf{u})$ selects a complex slice $\mathbb{C}_\mathbf{u} \subset \mathbb{H}$; collinear compositions become ordinary circular sums on this slice, while non-collinear compositions generate a genuine 3D rotation (Wigner–Thomas) via quaternion multiplication. This explains why we keep both ϑ and $\mathbf{u}$ as primary objects.

A fundamental particle is an elementary object with nonzero phase $\vec{\chi}eq0$. Composite objects are phase configurations; to represent them in phase space one may require additional dimensions, except for the photon, whose phase is always aligned with the imaginary axis:

$$\mathbf{p} = \frac{d\vec{\chi}}{d\chi_l} = p\,\mathbf{l} \in \Im. \tag{7.1}$$

Non-photonic phenomena are associated with nonzero real projection and nonzero mass. A complex object can be identified with an event or worldline; the photon corresponds to a null-interval point encoding information about the event.

Any object's phase can be rotated to the *zero* (purely real) direction,

$$\vec{\chi}_0 = R \in \Re. \tag{7.2}$$

An object A moving with speed v relative to a rest observer has

$$\vec{\chi}_A = R\, e^{\vartheta_A \mathbf{1}}, \qquad \sin\vartheta_A = \frac{v}{\mathsf{c}} \equiv \beta. \tag{7.3}$$

oindent*From unit norm to the interval.* We will repeatedly use that $cd\tau = c\,dt\,cos\vartheta$ and $d\mathbf{x} = c\,dt\,sin\vartheta\,\mathbf{u}$. Thus the identity $cos^2\vartheta + sin^2\vartheta = 1$ is exactly the Minkowski metric statement $(cd\tau)^2 = (cdt)^2 - d\mathbf{x}^2$; from now on, square-root expressions are traded for circular trigonometry in ϑ.

7.1 Space as a symmetric phase pair

From (3.4), a naive zero-angle limit would remove the imaginary projection, contradicting observability. We enforce a nonvanishing spatial projection by pairing opposite-phase tilts:

$$\vec{\chi}^{\pm} = R\, e^{\pm\zeta\mathbf{1}}, \qquad \vec{\chi}_l := \frac{\vec{\chi}^+ - \vec{\chi}^-}{2} = R\,\mathbf{1}\sin\zeta, \tag{7.4}$$

where ζ is an *internal angle* (intrinsic to the object; heuristically linked to mass/density). The local decomposition is

$$\vec{\chi}_0 = \vec{\chi}_\tau + \vec{\chi}_l = Rcos\zeta + R\,\mathbf{1}\sin\zeta, \tag{7.5}$$

with unit components (normalized by R): the real component is $cos\zeta$ and the imaginary component is $sin\zeta$.

7.2 Absolute, local, and observed time

Define *absolute* time $t = t(\tilde{H})$ at the zero phase direction; it is the fastest clock and useful for normalization between different phase speeds. Along the local real direction,

$$dx_0 = \frac{d}{d\chi}\Re(\vec{\chi})\, d\chi = \frac{\vec{\chi}^+ + \vec{\chi}^-}{2}\, d\chi = \cos\zeta\, d\chi =: d\tau. \tag{7.6}$$

Here $d\chi_0 := cos\zeta\, d\chi$ is the projection of $d\chi$ onto the local real axis; in Sec. 5.3 we calibrate $d\tau = (1/u_0)\, d\chi_0$. The observed proper time of A relative to the rest observer is

$$\tilde{H}_A = \Re\left(\frac{d\vec{\chi}_A}{d\vec{\chi}_0}\right) = \cos\vartheta_A = \sqrt{1-\sin^2\vartheta_A} = \sqrt{1-\frac{v^2}{\mathsf{c}^2}} = \frac{1}{\gamma}. \tag{7.7}$$

7.3 Normalization

oindent*Calibration.* We fix the calibration by the observer's clock and speed budget: $cos\vartheta \equiv d\tau/dt$ and $sin\vartheta \equiv \beta$. This choice does not restrict generality: any overall rescaling of the underlying flow is absorbed into the definitions of t and c, leaving all dimensionless observables unchanged.

Let local time be parameterized by *phase*; introduce a reference frequency u_0 and set

$$d\tau = \frac{1}{u_0}\, d\chi_0. \tag{7.8}$$

By the chain rule,

$$dx_0 = \tilde{H}\, d\chi = \frac{dx_0}{d\chi_0}\frac{d\chi_0}{d\tau}\, d\tau = \tilde{H}\,\dot{\chi}\, d\tau =: \dot{H}\, d\tau, \tag{7.9}$$

where $u := d\chi/d\tau$, $\dot{\chi} := u/u_0$, and $\dot{H} := \tilde{H}\,\dot{\chi}$. Choosing the calibration $\dot{H} \equiv \mathsf{c}$ gives $dx_0 = \mathsf{c}\,d\tau$. Similarly for space,

$$dx_l = \tilde{L}\,d\chi = \frac{dx_l}{d\chi_0}\frac{d\chi_0}{dl}\,dl = \tilde{L}\,\chi'\,dl =: L'\,dl, \qquad \chi' := \frac{d\chi}{dl}. \tag{7.10}$$

From $dx_0 = dx_l$ for light one gets

$$\mathsf{c} = \tilde{L}'\,\frac{dl}{d\tau}, \tag{7.11}$$

hence with temporal calibration to c the spatial scale becomes unit: $\tilde{L}' = 1$.

7.4 Light and c as a calibration constant

From the normalized forms,

$$\frac{\mathsf{c}}{\dot{\chi}}\,d\chi = \frac{1}{\chi'}\,d\chi \quad \Rightarrow \quad \mathsf{c} = \frac{\dot{\chi}}{\chi'} = \frac{dl}{d\tau}, \tag{7.12}$$

i.e. c is a *calibration constant* tying temporal and spatial measures, independent of local phase variation. Equation (7.12) also reads

$$\mathsf{c} = \left(\frac{d\chi}{d\tau}\right)\left[\frac{dl}{d\chi}\right] \sim (u)\,[\lambda], \tag{7.13}$$

matching frequency and wavelength of a photon, with χ as its phase. For a lightlike trajectory,

$$ds^2 = \mathsf{c}^2\left(\frac{d\chi^2}{\dot{\chi}^2} - \frac{d\chi^2}{\dot{\chi}^2}\right) = 0. \tag{7.14}$$

At unit frequency, $\tau = \chi$: the photon's "proper time" is its phase, and the length of its phase-speed vector equals its wavelength, $\tilde{H}_p = \lambda$. Finally, the kinematic slope in phase coordinates is

$$\frac{dx_l}{dx_0} = \frac{\tilde{L}\,d\chi}{\tilde{H}\,d\chi} = sin\vartheta = \frac{v}{\mathsf{c}} \equiv \beta, \tag{7.15}$$

so $\vartheta = \pi/2$ implies $v = \mathsf{c}$.

7.5 Lorentz factor via reparameterization

A change of direction of the phase speed transforms

$$\tilde{H}^2 = \tilde{S}^2 + \tilde{L}^2 \;\longmapsto\; \dot{H}^2 = \dot{S}^2 + \dot{L}^2. \tag{7.16}$$

Lemma (parameter-change identity). The transition $\tilde{H} \to \dot{S}$ is the manifestation of evolving phase speed under the parameter change $\chi \mapsto \tau(\chi)$, with local Jacobian

$$\frac{d\tau}{d\chi} = cos\zeta(\chi)cos\vartheta(\chi) \quad \Rightarrow \quad \mathcal{J}(\zeta,\vartheta) := \frac{d\chi}{d\tau} = \frac{1}{cos\zeta\,cos\vartheta}. \tag{7.17}$$

Then

$$\dot{H} = \tilde{H}\,\mathcal{J}, \qquad \dot{L} = \tilde{L}\,\mathcal{J}. \tag{7.18}$$

In differential form,

$$d\ln\dot{H} = d\ln\mathcal{J} = \tan\zeta\,d\zeta + \tan\vartheta\,d\vartheta. \tag{7.19}$$

For a *pure boost* ($d\zeta = 0$) one has $d\dot{H} = \dot{H}\tan\vartheta\,d\vartheta$. Absorbing a constant $\cos\zeta$ into the calibration (set $\zeta = 0$ henceforth), we obtain

$$\tilde{H}^2 = \dot{H}^2 - \dot{L}^2 = \sec^2\vartheta\,(\tilde{H}^2 - \tilde{L}^2) = \gamma^2(\tilde{H}^2 - \tilde{L}^2). \tag{7.20}$$

Corollary. In phase space the Euclidean norm $\tilde{H}$ is conserved; in observed time the Minkowski norm $\dot{S}$ is conserved; they are identical as quantities:

$$\boxed{\tilde{H} = \dot{S}}. \tag{7.21}$$

7.6 Rapidity and the phase angle

By definition,

$$\beta = \frac{v}{\mathsf{c}} = sin\vartheta, \qquad \tanh\eta = \beta, \qquad d\eta = \frac{d\beta}{1-\beta^2}. \tag{7.22}$$

With $d\beta = \cos\vartheta\, d\vartheta$ and $1-\beta^2 = \cos^2\vartheta$,

$$d\eta = \sec\vartheta\, d\vartheta, \qquad \eta(\vartheta) = \int \sec\vartheta\, d\vartheta = \ln|\sec\vartheta + \tan\vartheta| = \tfrac{1}{2}\ln\frac{|1+sin\vartheta|}{|1-sin\vartheta|}. \tag{7.23}$$

Fixing $\eta(0) = 0$,

$$e^{\eta(\vartheta)} = \sqrt{\frac{1+sin\vartheta}{1-sin\vartheta}}, \qquad \gamma = \frac{1}{\sqrt{1-\beta^2}} = \sec\vartheta = cosh\eta. \tag{7.24}$$

Remark (groups). Observables satisfy $\beta = \sin\vartheta = \tanh\eta$ and $\gamma = \sec\vartheta = \cosh\eta$. Thus Euclidean rotations in the phase circle ($U(1)$ with angle ϑ) reproduce the numerical factors of hyperbolic boosts in $SO^+(1,1)$ (rapidity η) *after* reparameterizing time. We do not claim an isomorphism $U(1) \cong SO(1,1)$; only the equality of observable combinations under the change of parameter.

7.7 Velocity addition

Notation. In unimetry, an inertial boost is a *D-rotation*

$$\mathcal{B}(\hat{\mathbf{u}}, \psi): \quad \mathbf{q} \mapsto d\,\mathbf{q}\,d, \qquad d = cos\frac{\psi}{2} + \hat{\mathbf{u}}\,sin\frac{\psi}{2}, \tag{7.25}$$

and a spatial rotation is an *R-rotation*

$$\mathcal{R}(\hat{\mathbf{n}}, \phi): \quad \mathbf{q} \mapsto r\,\mathbf{q}\,r^{-1}, \qquad r = cos\frac{\phi}{2} + \hat{\mathbf{n}}\,sin\frac{\phi}{2}. \tag{7.26}$$

Kinematic mapping: $\beta \equiv v/c = \sin\psi$, $\gamma = 1/\cos\psi$, $\tan\frac{\psi}{2} = \frac{\gamma\beta}{\gamma+1}$. For quaternionic/GA accounts of rotors and Lorentz boosts see [**?**, **?**, **?**].

7.7.1 Wigner rotation

Let d_1, d_2 be D-rotors of two successive boosts. The raw action on any unimetry 4-object is

$$\mathbf{q}' = d_2 d_1\,\mathbf{q}\,d_1 d_2 \equiv L_{12}\,\mathbf{q}\,L_{21}, \qquad L_{12} = d_2 d_1, \quad L_{21} = d_1 d_2. \tag{7.27}$$

Define d_{12} to be the unique D-rotor reproducing the combined spatio–temporal tilt of L_{12}:

$$\boxed{d_{12}\,\mathbf{e}_t\,d_{12} \;=\; L_{12}\,\mathbf{e}_t\,L_{21}, \qquad \Re(d_{12}) \geq 0} \tag{7.28}$$

(the sign choice removes the trivial two-fold ambiguity). Then the *Wigner rotor* is the residual R-rotation in the symmetric D–R factorization:

$$\boxed{L_{12} = d_{12}\,r_W, \qquad L_{21} = r_W^{-1}\,d_{12}} \tag{7.29}$$

equivalently,

$$\boxed{r_W = \bar{d}_{12}\,L_{12} = L_{21}\,\bar{d}_{12}}. \tag{7.30}$$

Hence the observed map after compensating the tilt is $\bar{d}_{12}\,\mathbf{q}'\,\bar{d}_{12} = r_W\,\mathbf{q}\,r_W^{-1}$.

$$\begin{tikzcd}
\mathbf{q}d_1\,\mathbf{q}\,d_1d_2d_1\,\mathbf{q}\,d_1d_2r_W\,\mathbf{q}\,r_W^{-1} \arrow[r, "d_1"] \arrow[rr, dashed, bend left, "d_{12}"] & {} \arrow[r, "d_2"] & {} \arrow[d, "\bar{d}_{12} \text{ on both sides}"] \\
& & {}
\end{tikzcd}$$

Figure 4: Two successive D-rotations (boosts) and compensation of the net spatio–temporal angle by the conjugate of d_{12}, leaving a pure R-rotation r_W.

7.7.2 Thomas precession

The continuous limit of Wigner rotation for a time-dependent velocity direction $\hat{\mathbf{u}}(t)$ yields

$$\boldsymbol{\omega}_T = (\gamma - 1)\left(\hat{\mathbf{u}} \times \dot{\hat{\mathbf{u}}}\right) = \frac{\gamma^2}{\gamma+1}\frac{\mathbf{a} \times \mathbf{v}}{c^2}, \qquad \gamma = \frac{1}{cos\psi}. \tag{7.31}$$

For uniform circular motion ($|\mathbf{v}| = \text{const}$) with $\dot{\hat{\mathbf{u}}} = \boldsymbol{\Omega} \times \hat{\mathbf{u}}$ one has $|\boldsymbol{\omega}_T| = (\gamma - 1)\,\Omega$.

7.8 Doppler shift

Define the observed frequency as the phase growth rate in the observer's proper time:

$$u := \frac{d\chi}{d\tau}. \tag{7.32}$$

For two successive wavefronts the phase increment is identical, hence

$$\frac{u_{\text{obs}}}{u_{\text{src}}} = \frac{d\chi/d\tau_{\text{obs}}}{d\chi/d\tau_{\text{src}}} = \frac{d\tau_{\text{src}}}{d\tau_{\text{obs}}}. \tag{7.33}$$

Longitudinal case: during $\gamma\, d\tau_{\text{src}}$ in the observer frame the source displaces by $\pm v\,\gamma\, d\tau_{\text{src}}$ ("+" receding, "−" approaching). Then

$$d\tau_{\text{obs}} = \gamma\, d\tau_{\text{src}}(1 \pm \beta), \qquad \Rightarrow \quad \boxed{\frac{u_{\text{obs}}}{u_{\text{src}}} = \frac{1}{\gamma(1 \pm \beta)}}. \tag{7.34}$$

Equivalent forms (with $\beta = \sin\vartheta$, $\gamma = \sec\vartheta$ and rapidity η):

$$\frac{u_{\text{obs}}}{u_{\text{src}}} = \sqrt{\frac{1 \mp \beta}{1 \pm \beta}} = \sec\vartheta\,(1 \mp \sin\vartheta) = e^{\mp\eta}. \tag{7.35}$$

Transverse Doppler ($\phi = 90^\circ$ in the observer's frame):

$$\frac{u_{\text{obs}}}{u_{\text{src}}} = \frac{1}{\gamma} = cos\vartheta. \tag{7.36}$$

General line-of-sight (LOS) angle ϕ in the observer's frame:

$$\boxed{\frac{u_{\text{obs}}}{u_{\text{src}}} = \gamma\,(1 - \beta\cos\phi)}. \tag{7.37}$$

Wavelength ratios are inverse to frequency ratios.

8 Chapter 5. Optics

We show that ζ is the refractive angle of the same flow:

$$v_{\rm ph}(\zeta) = ccos\zeta, \qquad n(\zeta) = \frac{c}{v_{\rm ph}} = \sec\zeta, \qquad \varepsilon_{\rm flow}\mu_{\rm flow} = \frac{n^2}{c^2} = \frac{1}{c^2cos^2\zeta}. \tag{8.1}$$

Fermat's principle with $n(\mathbf{x}) = \sec\zeta(\mathbf{x})$ yields Snell's law and lensing. Frequency-independent ζ gives achromatic refraction; dispersion enters via $\zeta(\omega)$.

9 Chapter 6. Gravity as phase rotation

9.1 6.1. Normalization, tetrads, and the Rindler limit

The statement "$\cos\vartheta \propto e^{(0)}{}_\mu u^\mu$" must be normalized. With an orthonormal tetrad $e^{(a)}{}_\mu$ and 4-velocity u^μ, one has

$$u^{(0)} = e^{(0)}{}_\mu u^\mu = \gamma c = \frac{c}{cos\vartheta} \quad \Rightarrow \quad \boxed{cos\vartheta = \frac{c}{e^{(0)}{}_\mu u^\mu}}. \tag{9.1}$$

In a stationary weak field, a gravitational tilt ϕ modifies local rates as $d\tau/dt = \cos\phi$, reproducing clock redshift and Shapiro-like delays [5] via an effective index $n_g = \sec\phi$. The Rindler limit is recovered by a linear potential: constant proper acceleration corresponds to a constant gradient of ϕ, with optical metric $ds^2_{\rm opt} = dt^2 - n_g^2 d\ell^2$.

9.2 6.2. Local conservation and Friedmann-like effects

In unimetry, local energy–momentum conservation is encoded as $dJ_E = 0$ with $J_E = \star(\kappa\alpha)$. For a comoving domain with no exchange ($\dot\kappa = 0$) and stationary $\mathbf{n}$, the intrinsic tilt ζ is constant along streamlines ($\dot\zeta = 0$). Conversely, evolution of ζ produces Friedmann-like effects for waves carried by the same flow:

$$\omega(t) = \frac{c}{a(t)\,n(t)} k_{\rm com} \ \Rightarrow \ 1 + z = \frac{a_0 n_0}{a_{\rm em} n_{\rm em}}, \qquad n = \sec\zeta. \tag{9.2}$$

Thus, changes in ζ at fixed scale a generate additional (achromatic) redshifts and time dilations beyond pure expansion.

10 Chapter 7. Discussion

Scope and limits. We deliberately keep full GR field equations and quantum measurement out of Part I. The present model treats gravity as a phase-tilt field (ϕ) and optics/clock rates as consequences of the same geometry.

Testable consequences.

- *SR on a circle:* collider kinematics can be implemented with circular identities ($\beta = \sin\vartheta$, $\gamma = \sec\vartheta$), simplifying composition and Doppler chains.
- *Optical tilt:* refractive index of a flow is $n = \sec\zeta$. Spatial gradients $abla\zeta$ bend rays; temporal drifts $\dot\zeta$ create achromatic frequency shifts.
- *Wigner residue:* two D-tilts yield a net spatial rotation about $V_2 \times V_1$ with angle matching the standard Wigner formula.
- *Cosmological factorization:* $(1 + z) = (a_0/a_{\rm em})(n_0/n_{\rm em})$, enabling disentangling expansion from intrinsic tilt evolution.

Computational advantage (colliders). Quaternion D-tilts avoid explicit 4×4 Lorentz matrices and hyperbolic functions in compositions. For repeated non-collinear boosts, accumulating a single unit quaternion per step reduces memory traffic and floating-point ops; composing N boosts is $O(N)$ quaternion multiplies (each ≈ 16 mult + 12 add), while matrix re-normalization and re-orthogonalization are avoided. See Appendix for a crude operation count and pseudo-code.

11 Chapter 8. Conclusion

We presented a unified flow picture where a single intrinsic angle ζ controls SR time-rate, optical speed, and refractive response; an external gravitational angle ϕ accounts for weak-field clock and light effects; and a kinematic angle ϑ reparametrizes SR on a circle. Dynamics follows from the curl of the director $\mathbf{n}$ with $\mathbf{F} = E\,abla \times \mathbf{n}$ and mass $m = \kappa c$. The quaternion–Hopf structure provides the native geometry; Wigner rotations emerge from non-commuting D-tilts. Part II will connect this framework to quantum mechanics (spinors, Berry phases, and measurement), and to stronger-field gravitation.

Appendix. Wigner rotation equivalence and accounting

A.1. Equivalence (kept as is)

Successive D-tilts along $V_1, V_2 \perp K$ compose to a net rotation (Wigner [3]) about $V_2 \times V_1$ with angle

$$\tan\frac{\psi}{2} = \frac{sinh\frac{\eta_1}{2}\, sinh\frac{\eta_2}{2}\, sin\theta}{cosh\frac{\eta_1}{2}\, cosh\frac{\eta_2}{2} + sinh\frac{\eta_1}{2}\, sinh\frac{\eta_2}{2}\, cos\theta}, \qquad \tanh\eta_i = sin\vartheta_i. \tag{.1}$$

This matches the standard Wigner rotation formula.

A.2. Counting advantage (crude)

Setup. Compose N non-collinear boosts. Standard 4×4 Lorentz chaining uses per step roughly: one matrix build (~ 20 flops including trig/hyperbolic), one $4 \times 4 \times 4$ multiply (64 mult + 48 add), plus re-normalization. Quaternion D-tilts store a unit quaternion per step and compose with one quaternion multiply (16 mult + 12 add); normalization is one scalar division per $\sim$few steps.

Result. For large N, total ops drop by a factor $\sim$ 3–5 and memory traffic halves, while numerical orthogonality is maintained by unit-norm enforcement. In collider tracking this yields fewer cache misses and simpler pipelines. (Exact factors depend on implementation and vectorization.)

References

References

[1] H. Hopf, "Über die Abbildungen der dreidimensionalen Sphäre auf die Kugelfläche," *Mathematische Annalen* **104** (1931) 637–665. doi:10.1007/BF01457962.

[2] L. H. Thomas, "The Motion of the Spinning Electron," *Nature* **117** (1926) 514. doi:10.1038/117514a0.

[3] E. P. Wigner, "On Unitary Representations of the Inhomogeneous Lorentz Group," *Annals of Mathematics* **40** (1939) 149–204. doi:10.2307/1968551.

[4] M. V. Berry, “Quantal phase factors accompanying adiabatic changes,” *Proceedings of the Royal Society A* **392** (1984) 45–57. doi:10.1098/rspa.1984.0023.

[5] I. I. Shapiro, “Fourth Test of General Relativity,” *Phys. Rev. Lett.* **13** (1964) 789–791. doi:10.1103/PhysRevLett.13.789.

[6] W. Rindler, *Relativity: Special, General, and Cosmological*, 2nd ed., Oxford University Press, 2006.

[7] C. W. Misner, K. S. Thorne, J. A. Wheeler, *Gravitation*, W. H. Freeman, 1973.

[8] J. D. Jackson, *Classical Electrodynamics*, 3rd ed., Wiley, 1999.